A capable numerical meshless scheme for solving distributed order time-fractional reaction-diffusion equation

Esmail Hesameddini[1], Ali Habibirad[1], and Hadis Azin[2]

[1]Shiraz University of Technology
[2]Hormozgan University of Medical Sciences

August 16, 2022

Abstract

Distributed order fractional differential equations are efficient in describing physical phenomena because of the differential order distribution. In this paper, the distributed order time-fractional reaction-diffusion equation is considered in the sense of Caputo fractional derivative. A hybrid method is developed based on the Moving Kriging (MK) interpolation and finite difference method for solving this distributed order equation. First, the distributed integral is discretized by the M-point Gauss Legendre quadrature rule. Then, the $L2-1_{\sigma}$ method is applied to approximate the solution of the fractional derivative discretization. Also, the unconditionally stability and rate of convergence $O(\tau^{2})$ of the time-discrete technique are illustrated. Furthermore, the MK interpolation is applied in the space variables discretization. Finally, some examples are presented to indicate the efficiency of this method and endorsement the theoretical results.

1

A capable numerical meshless scheme for solving distributed order time-fractional reaction-diffusion equation

Ali Habibirad[1], Hadis Azin[2] and Esmail Hesameddini[1]

[1] *Department of Mathematics, Shiraz University of Technology, Shiraz, Iran.*

[2] *Department of Mathematics, University of Hormozgan, Bandar Abbas, Iran*

Abstract

Distributed order fractional differential equations are efficient in describing physical phenomena because of the differential order distribution. In this paper, the distributed order time-fractional reaction-diffusion equation is considered in the sense of Caputo fractional derivative. A hybrid method is developed based on the Moving Kriging (MK) interpolation and finite difference method for solving this distributed order equation. First, the distributed integral is discretized by the M-point Gauss Legendre quadrature rule. Then, the $L2-1_\sigma$ method is applied to approximate the solution of the fractional derivative discretization. Also, the unconditionally stability and rate of convergence $O(\tau^2)$ of the time-discrete technique are illustrated. Furthermore, the MK interpolation is resulted in the space variables discretization. Finally, some examples are presented to indicate the efficiency of this method and endorsement the theoretical results.

Keywords: Distributed order fractional derivative, Time-fractional reaction diffusion equation, Moving Kriging interpolation, Finite difference.
2000 MSC: 65M12,65M60, 34A45.

1. Introduction

Fractional calculus is a field of mathematics that is obtained from definitions of calculus integral and derivative operators with arbitrary order. In the last few decades, fractional calculus has been used in science and many branches of engineering [1, 2, 3, 4, 5, 6, 7]. The importance of fractional calculus led to the study of various fractional differential equations (FDEs) analytically and numerically [8, 9]. For example, Nauman and co-authors investigated a fractional-order system of malaria pestilence with the stability of the model at equilibrium points in [10]. GPU-based modeling is considered with a parallel fractional-order derivative

---

*Corresponding author Email: hesameddini@sutech.ac.ir

Email address: `a.habibirad@sutech.ac.ir,hesameddini@sutech.ac.ir` (Ali Habibirad[1], Hadis Azin[2] and Esmail Hesameddini[1])

in [11]. The boundary-value problems containing fractional derivatives and fractional integral boundary conditions were considered in [12]. Also, different definitions of fractional derivatives were used in FDEs [13]. To investigate some definitions of fractional derivatives, the interested readers are referred to [14, 15, 16, 17]. The distributed order operator is to be a middleman between fractional-order and integer-order operators [18]. The generality of the single order and multiterm fractional differential equations is the cause of the distributed order fractional differential equations [19]. Caputo [20] employed the distributed-order FDEs to generalize the stress-strain connection in dielectrics. Bagley and Torvik [21, 22] used distributed-order derivatives to deliver samples of the input-output connection of a linear time-variant procedure according to commonness domain statements. This model was utilized in designing the movement of a strict plate submerged in a Newtonian fluid concerning the nonnegative density function [23]. The time distributed-order fractional models can describe procedures that don't have a power-law scale on the entire time-domain [24], such as the ultraslow distribution where a mass of particles is scattered at a logarithmic velocity [25]. To observe other details of distributed-order fractional equations the readers could see [26] and the references therein. In this study, we assume the distributed order time-fractional reaction-diffusion model as follows

$$\int_0^1 \varpi(\alpha)\, {}_0^c D_t^\alpha u(\mathbf{x},t)d\alpha - \Delta u(\mathbf{x},t) + u(\mathbf{x},t) = f(\mathbf{x},t), \qquad \mathbf{x} = (x_1,\ldots,x_d) \in \Omega \subseteq \mathbb{R}^d, \qquad 0 \leq t \leq T, \ (1.1)$$

with $d = 1, 2$ and the initial and boundary conditions

$$\begin{cases} u(\mathbf{x},0) = u_0(\mathbf{x}), \\ u(\mathbf{x},t) = \Psi(\mathbf{x},t), \quad \mathbf{x} \in \partial\Omega. \end{cases} \tag{1.2}$$

In this equation ${}_0^c D_t^\alpha u(\mathbf{x},t)$ denotes the Caputo fractional derivative of $u(\mathbf{x},t)$ which for $\alpha = 1$ equal first derivative and

$$_0^c D_t^\alpha u(\mathbf{x},t) = \frac{1}{\Gamma(1-\alpha)} \int_0^t \frac{\partial u(\mathbf{x},s)}{\partial s} \frac{ds}{(t-s)^\alpha}, \qquad 0 < \alpha < 1, \tag{1.3}$$

where $\Gamma(.)$ is Euler's Gamma function and Δ is the d-dimensional Laplace differential operator. Also, the continuous weight function $\varpi(\alpha)$ has the following conditions

$$\begin{cases} \varpi(\alpha) > 0, \\ 0 < \int_0^1 \varpi(\alpha)d\alpha < \infty. \end{cases} \tag{1.4}$$

Some researchers studied the distributed order time-fractional diffusion model. In [27], a finite difference/spectral approach was presented for the numerical solution of a distributed order time-fractional diffusion model with initial singularity on a two-dimensional spatial domain. The authors of [28] generated and analyzed an efficient finite-difference/generalized Hermite spectral approach for solving the distributed-order time-fractional reaction-diffusion equation on multidimensional cases with unbounded domains. The main aim of [29] was to present an efficient numerical formulation for the numerical solution of this model with local radial basis function and finite difference method. In [30], the authors applied the Laplace transform

2

scheme to obtain a new operational vector for the Riemann Liouville fractional integral of the Müntz-Legendre wavelets. In [31] Legendre wavelet method has been suggested for linear and nonlinear distributed FDEs. Ding et al. [32] proposed a second-order numerical scheme for the Riemann-Liouville tempered fractional derivative with tempered Grünwald difference operator and its asymptotic expansion. Moghaddam and co-authors [33] discussed a numerical approximation based on a linear B-spline scheme and the mid-point quadrature rule to solve distributed-order PDEs. In [34] Jacobi-Gauss-Lobatto collocation technique was used for the numerical solution of the Schrödinger equation with distributed-order time and Riesz space-fractional. To see the more numerical scheme for distributed order FDEs see [29] and references therein. In the present research study, the shape functions of the moving Kriging method will be applied to space discretization. The new approximation scheme is collocation and local numerical technique. Similarly, this method is a meshless scheme and can be used for numerical solution of different PDEs on regular and irregular domains in one and two-dimensional types.

The rest of this article is formed as follows. In Section 2, some basic Preliminary are presented. In section 3, we construct the semi-discrete scheme for the distributed-order fractional term and the time variable. Also, the stability and the convergence order of this scheme are investigated. The MK interpolation method has been explained in Section 4 and implemented for the problem in Section 5 under study. In Section 6 some examples are solved by the proposed method. The article ends with a conclusion in Section 7.

2. Preliminary

In this section, some definitions and preliminaries are explained.

Definition 2.1. Let $d\mathbf{x}$ is the Lebesgue measure on $\mathbb{R}^d$. Then, $L^2(\Omega)$ is the space of all measurable functions $g : \Omega \longrightarrow \mathbb{R}$ such that

$$\int_\Omega |g(\mathbf{x})|^2 d\mathbf{x} < \infty. \tag{2.1}$$

The $L^2(\Omega)$ is a Hilbert space with the inner product

$$\langle g, h \rangle = \int_\Omega g(\mathbf{x}) h(\mathbf{x}) d\mathbf{x}, \tag{2.2}$$

and the following norm,

$$\|g\| = \left(\int_\Omega \left(g(\mathbf{x}) \right)^2 d\mathbf{x} \right)^{\frac{1}{2}}. \tag{2.3}$$

In this study, we consider the real-valued functions space as

$$H^1(\Omega) = \{ g : \Omega \longrightarrow \mathbb{R} | \quad g \quad \text{and} \quad g_\mathbf{x} \in L^2(\Omega) \}, \qquad H_0^1(\Omega) = \{ g \in H^1(\Omega), \ g|_{\partial\Omega} = 0 \}. \tag{2.4}$$

Definition 2.2. Let $J \in C^\infty([-1, 1])$, the M-point Gaussian-Legendre integration is given by

$$\int_{-1}^1 J(x)dx = \sum_{j=1}^M \tilde{\omega}_j J(p_j) + \frac{2^{2M+1}(M!)^4}{(2M+1)((2M)!)^3} \frac{d^{2M}J(x)}{dx^{2M}}, \tag{2.5}$$

where

$$\tilde{\omega}_j = \frac{2}{(1-p_j^2)\left(L'_M(p_i)\right)^2}, \tag{2.6}$$

are weights Gauss-Legendre quadrature and p_j are roots of Legendre polynomial $L_M(x)$ in $[-1, 1]$.

So, the integral term in (1.1) will be approximated via the Gauss-Legendre quadrature rule as

$$\int_0^1 \varpi(\alpha) \, {}_0^c D_t^\alpha u(\mathbf{x}, t)d\alpha = \sum_{j=1}^M \frac{1}{2}\tilde{\omega}_j \varpi(\alpha_j) \, {}_0^c D_t^{\alpha_j} u(\mathbf{x}, t) + O(4^{-M}), \tag{2.7}$$

in which $\alpha_j = \dfrac{p_j + 1}{2}$.

3. Time discretization

3.1. Time discretization scheme

To construct the finite difference technique for the distributed order fractional (1.1), let $\tau = \dfrac{T}{n_t}$ be the step size of time and define $t_n = n\tau$, $n = 0, 1, 2, \cdots, n_t$. The Caputo fractional derivative ${}_0^c D_t^{\alpha_j} u(\mathbf{x}, t)$ in Eq. (2.7) is approximated by the $L2 - 1_\sigma$ method [28] in which $\sigma \in [\frac{1}{2}, 1]$ as follows

$$\,{}_0^c D_t^{\alpha_j} u(\mathbf{x}, t_{n+\sigma}) = \sum_{l=0}^n \frac{\tau^{-\alpha_j}}{\Gamma(2-\alpha_j)} c_l^{(n+1,\alpha_j)} \left(u(\mathbf{x}, t_{n-l+1}) - u(\mathbf{x}, t_{n-l})\right) + O(\tau^{3-\alpha_{\max}}), \tag{3.1}$$

where

$$c_l^{(n+1,\alpha_j)} = \begin{cases} \dfrac{1}{2-\alpha_j}[(1+\sigma)^{2-\alpha_j} - \sigma^{2-\alpha_j}] - \dfrac{1}{2}[(1+\sigma)^{1-\alpha_j} - \sigma^{\alpha_j}], & l = 0, \\[2mm] (l+\sigma)^{1-\alpha_j} - \dfrac{1}{2}[(l+1+\sigma)^{1-\alpha_j} + (l+1+\sigma)^{1-\alpha_j}] & l = 1, \cdots, n-1, \\[1mm] \quad + \dfrac{1}{2-\alpha_j}[(l+1+\sigma)^{2-\alpha_j} - 2(l+\sigma)^{2-\alpha_j} + (l-1+\sigma)^{2-\alpha_j}], & \\[2mm] \dfrac{1}{2}[3(l+\sigma)^{1-\alpha_j} - (l-1+\sigma)^{1-\alpha_j}] - \dfrac{1}{2-\alpha_j}[(l+\sigma)^{2-\alpha_j} - (l-1+\sigma)^{2-\alpha_j}], & l = n. \end{cases} \tag{3.2}$$

Also,

$$u(\mathbf{x}, t) = \sigma u(\mathbf{x}, t_{n+1}) + (1-\sigma)u(\mathbf{x}, t_n). \tag{3.3}$$

4

Substituting (2.7), (3.1) and (3.3) in (1.1), results in

$$\sum_{l=0}^{n} d_l^{(n+1)}\Big(u(\mathbf{x},t_{n-l+1}) - u(\mathbf{x},t_{n-l})\Big) - \Delta\big(\sigma u(\mathbf{x},t_{n+1}) + (1-\sigma)u(\mathbf{x},t_n)\big)$$
$$+ \sigma u(\mathbf{x},t_{n+1}) + (1-\sigma)u(\mathbf{x},t_n) = f(\mathbf{x},t_{n+\sigma}) + O(4^{-M} + \tau^{3-\alpha_{\max}}),$$
(3.4)

where $d_l^{(n+1)} = \sum_{j=1}^{M} \dfrac{\tau^{-\alpha_j}}{2\Gamma(2-\alpha_j)}\tilde{\omega}_j\varpi(\alpha_j)c_l^{(n+1,\alpha_j)}$. Moreover, there is a constant $C > 0$ such that $\xi_\alpha^n < C\tau^{3-\alpha_{\max}}$. Eliminating the small term ξ_α^n, yields

$$\sum_{l=0}^{n} d_l^{(n+1)}\Big(\tilde{u}(\mathbf{x},t_{n-l+1}) - \tilde{u}(\mathbf{x},t_{n-l})\Big) - \Delta\big(\sigma\tilde{u}_{n+1} + (1-\sigma)\tilde{u}_n\big) + \sigma\tilde{u}_{n+1} + (1-\sigma)\tilde{u}_n = f_{n+\sigma}, \quad (3.5)$$

where $\tilde{u}_n = \tilde{u}(\mathbf{x},t_n)$ is an approximation of the exact solution $u(\mathbf{x},t_n)$.

3.2. Stability and convergence of time discretization scheme

In this section, the stability and order of convergence analysis for the semi-discrete scheme (3.5) will be demonstrated.

REMARK 1. Simplifying relation (3.4), one obtains

$$\sum_{l=0}^{n+1} e_l^{(n+1)}u(\mathbf{x},t_l) - \Delta\big(\sigma u(\mathbf{x},t_{n+1}) + (1-\sigma)u(\mathbf{x},t_n)\big) + \sigma u(\mathbf{x},t_{n+1}) + (1-\sigma)u(\mathbf{x},t_n) = f(\mathbf{x},t_{n+\sigma}) + \xi_\alpha^n, \quad (3.6)$$

where

$$e_l^{(n+1)} = \begin{cases} e_1^{(1)} = -e_0^{(1)} = d_0^{(1)}, & n = 0, \\ \begin{cases} -d_n^{(n+1)}, & l = 0, \\ d_{n-l+1}^{(n+1)} - d_{n-l}^{(n+1)}, & l = 1,\cdots,n, \\ d_0^{(n+1)}, & l = n+1. \end{cases} & n \geq 1, \end{cases} \quad (3.7)$$

Lemma 3.1. *([35]) For $n \in \mathbb{N} \cup \{0\}$, we have*

$$e_0^{(1)} < 0, \qquad e_l^{(n+1)} < 0, \qquad l = 0,1,\cdots,n, \quad (3.8)$$

and

$$\sum_{l=0}^{n+1} e_l^{(n+1)} = 0, \qquad e_{n+1}^{(n+1)} > 0. \quad (3.9)$$

Theorem 3.2. *The semi-discrete procedure (3.6) is unconditionally stable and there is a constant $C > 0$ such that*

$$\|\tilde{u}_{n+1}\| \leq C \max_{0 \leq n \leq n_t} \|f_{n+\sigma}\|. \quad (3.10)$$

Proof. Taking the inner product $v = \sigma \tilde{u}_{n+1} + (1 - \sigma)\tilde{u}_n \in H_0^1(\Omega)$ in (3.6), we get

$$\sum_{l=0}^{n+1} e_l^{(n+1)} \int_\Omega \tilde{u}_l(\sigma \tilde{u}_{n+1} + (1 - \sigma)\tilde{u}_n)d\mathbf{x} - \int_\Omega \Delta\big(\sigma \tilde{u}_{n+1} + (1 - \sigma)\tilde{u}_n\big)(\sigma \tilde{u}_{n+1} + (1 - \sigma)\tilde{u}_n)d\mathbf{x}$$
$$+ \|\sigma \tilde{u}_{n+1} + (1 - \sigma)\tilde{u}_n\|^2 = \int_\Omega f_{n+\sigma}(\sigma \tilde{u}_{n+1} + (1 - \sigma)\tilde{u}_n)d\mathbf{x}. \tag{3.11}$$

Using the integration by parts and boundary condition (3.11), results in

$$\sum_{l=0}^{n+1} e_l^{(n+1)} \int_\Omega \tilde{u}_l(\sigma \tilde{u}_{n+1} + (1 - \sigma)\tilde{u}_n)d\mathbf{x} + \|\nabla\big(\sigma \tilde{u}_{n+1} + (1 - \sigma)\tilde{u}_n\big)\|^2 + \|\sigma \tilde{u}_{n+1} + (1 - \sigma)\tilde{u}_n\|^2$$
$$= \int_\Omega f_{n+\sigma}(\sigma \tilde{u}_{n+1} + (1 - \sigma)\tilde{u}_n)d\mathbf{x}. \tag{3.12}$$

Obviously $\|\nabla\big(\sigma \tilde{u}_{n+1} + (1 - \sigma)\tilde{u}_n\big)\|^2 \geq 0$ and $\|\sigma \tilde{u}_{n+1} + (1 - \sigma)\tilde{u}_n\|^2 \geq 0$. Then, one obtains

$$e_{n+1}^{(n+1)} \Big\langle \tilde{u}_{n+1}, \sigma \tilde{u}_{n+1} + (1 - \sigma)\tilde{u}_n \Big\rangle \leq -\sum_{l=0}^{n} e_l^{(n+1)} \int_\Omega \tilde{u}_l(\sigma \tilde{u}_{n+1} + (1 - \sigma)\tilde{u}_n)d\mathbf{x}$$
$$+ \int_\Omega f_{n+\sigma}(\sigma \tilde{u}_{n+1} + (1 - \sigma)\tilde{u}_n)d\mathbf{x}. \tag{3.13}$$

The inequality (3.13) can be rewritten as

$$e_{n+1}^{(n+1)} \Big\langle \tilde{u}_{n+1}, \sigma \tilde{u}_{n+1} + (1 - \sigma)\tilde{u}_n \Big\rangle = e_{n+1}^{(n+1)} \frac{1}{\sigma} \int_\Omega \sigma\Big(\tilde{u}_{n+1} - (1 - \sigma)\tilde{u}_n + (1 - \sigma)\tilde{u}_n\Big)(\sigma \tilde{u}_{n+1} + (1 - \sigma)\tilde{u}_n)d\mathbf{x}$$
$$= \frac{e_{n+1}^{(n+1)}}{\sigma}\Big(\|\sigma \tilde{u}_{n+1}\|^2 - \|(1 - \sigma)\tilde{u}_n\|^2 + (1 - \sigma)\int_\Omega \tilde{u}_n\big(\sigma \tilde{u}_{n+1} + (1 - \sigma)\tilde{u}_n\big)d\mathbf{x}\Big)$$
$$\leq -\sum_{l=0}^{n} e_l^{(n+1)} \int_\Omega \tilde{u}_l(\sigma \tilde{u}_{n+1} + (1 - \sigma)\tilde{u}_n)d\mathbf{x} + \int_\Omega f_{n+\sigma}(\sigma \tilde{u}_{n+1} + (1 - \sigma)\tilde{u}_n)d\mathbf{x}.$$
$$\tag{3.14}$$

Considering the Cauchy-Schwarz inequality, we have

$$\frac{e_{n+1}^{(n+1)}}{\sigma}\|\sigma \tilde{u}_{n+1}\|^2 - \frac{e_{n+1}^{(n+1)}}{\sigma}\|(1 - \sigma)\tilde{u}_n\|^2 \leq -\frac{e_{n+1}^{(n+1)}}{\sigma}\int_\Omega (1 - \sigma)\tilde{u}_n\big(\sigma \tilde{u}_{n+1} + (1 - \sigma)\tilde{u}_n\big)$$
$$- \sum_{l=0}^{n}\Big(e_l^{(n+1)} \int_\Omega \tilde{u}_l(\sigma \tilde{u}_{n+1} + (1 - \sigma)\tilde{u}_n)d\mathbf{x}\Big) + \|f_{n+\sigma}\|\|\sigma \tilde{u}_{n+1} + (1 - \sigma)\tilde{u}_n\|$$
$$= \sum_{l=0}^{n} \int_\Omega (-e_l^{(n+1)}\tilde{u}_l - \frac{e_{n+1}^{(n+1)}}{\sigma}(1 - \sigma)\tilde{u}_n)(\sigma \tilde{u}_{n+1} + (1 - \sigma)\tilde{u}_n)d\mathbf{x}$$
$$+ \|f_{n+\sigma}\|\|\sigma \tilde{u}_{n+1} + (1 - \sigma)\tilde{u}_n\|. \tag{3.15}$$

For simplicity, we define

$$\hat{e}_l^{(n+1)} = \begin{cases} -e_0^{(1)}, & n = 0, \\ \begin{cases} -e_l^{(n+1)}, & l = 0, \cdots, n-1, \\ -e_n^{(n+1)} - \dfrac{e_{n+1}^{(n+1)}}{\sigma}(1-\sigma), & l = n, \end{cases} & n \geq 1, \end{cases} \tag{3.16}$$

considering Lemma 3.1, $\hat{e}_l^{(n+1)} > 0$. Therefore, applying the relation (3.16) and Cauchy-Schwarz in (3.15), results in

$$\begin{aligned} \frac{e_{n+1}^{(n+1)}}{\sigma}\|\sigma\tilde{u}_{n+1}\|^2 - \frac{e_{n+1}^{(n+1)}}{\sigma}\|(1-\sigma)\tilde{u}_n\|^2 &\leq \sum_{l=0}^{n} \hat{e}_l^{(n+1)} \int_\Omega \tilde{u}_l(\sigma\tilde{u}_{n+1} + (1-\sigma)\tilde{u}_n)d\mathbf{x} \\ &\quad + \|f_{n+\sigma}\|\|\sigma\tilde{u}_{n+1} + (1-\sigma)\tilde{u}_n\| \\ &\leq \sum_{l=0}^{n} \hat{e}_l^{(n+1)}\|\tilde{u}_l\|\|\sigma\tilde{u}_{n+1} + (1-\sigma)\tilde{u}_n\| \\ &\quad + \|f_{n+\sigma}\|\|\sigma\tilde{u}_{n+1} + (1-\sigma)\tilde{u}_n\| \\ &= \left(\sum_{l=0}^{n} \hat{e}_l^{(n+1)}\|\tilde{u}_l\| + \|f_{n+\sigma}\|\right)\left(\|\sigma\tilde{u}_{n+1} + (1-\sigma)\tilde{u}_n\|\right). \end{aligned} \tag{3.17}$$

Multiplying the both sides of (3.17) by $\dfrac{1}{\sigma e_{n+1}^{(n+1)}}$, yields

$$\|\tilde{u}_{n+1}\|^2 - \|\frac{(1-\sigma)}{\sigma}\tilde{u}_n\|^2 \leq \frac{1}{e_{n+1}^{(n+1)}}\left(\sum_{l=0}^{n} \hat{e}_l^{(n+1)}\|\tilde{u}_l\| + \|f_{n+\sigma}\|\right)\left(\|\tilde{u}_{n+1} + \frac{(1-\sigma)}{\sigma}\tilde{u}_n\|\right). \tag{3.18}$$

This inequality can be rewritten as

$$\|\tilde{u}_{n+1}\| - \|\frac{(1-\sigma)}{\sigma}\tilde{u}_n\| \leq \frac{1}{e_{n+1}^{(n+1)}}\sum_{l=0}^{n} \hat{e}_l^{(n+1)}\|\tilde{u}_l\| + \frac{1}{e_{n+1}^{(n+1)}}\|f_{n+\sigma}\|. \tag{3.19}$$

So,

$$\|\tilde{u}_{n+1}\| \leq \|\frac{(1-\sigma)}{\sigma}\tilde{u}_n\| + \frac{1}{e_{n+1}^{(n+1)}}\sum_{l=0}^{n} \hat{e}_l^{(n+1)}\|\tilde{u}_l\| + \frac{1}{e_{n+1}^{(n+1)}}\|f_{n+\sigma}\|. \tag{3.20}$$

For $n = 0$, according to the relation (3.7) and Grönwall's inequality, we have

$$\begin{aligned} \|\tilde{u}_1\| &\leq \|\frac{(1-\sigma)}{\sigma}\tilde{u}_0\| + \frac{-e_0^{(1)}}{e_1^{(1)}}\|\tilde{u}_0\| + \frac{1}{e_1^{(1)}}\|f_\sigma\| = \|\frac{(1-\sigma)}{\sigma}\tilde{u}_0\| + \|\tilde{u}_0\| + \frac{1}{e_1^{(1)}}\|f_\sigma\| \\ &\leq \|\tilde{u}_0\| + \frac{1}{e_1^{(1)}}\|f_\sigma\| \leq \frac{\exp(2\tau)}{e_1^{(1)}} \max_{0 \leq n \leq n_t} \|f_{n+\sigma}\| \leq C_0 \max_{0 \leq n \leq n_t} \|f_{n+\sigma}\|. \end{aligned} \tag{3.21}$$

For $n \geq 1$, the Lemma 3.1 and the Grönwall's inequality, implies that

$$
\begin{aligned}
\|\tilde{u}_{n+1}\| &\leq \|\frac{(1-\sigma)}{\sigma}\tilde{u}_n\| + \frac{1}{e_{n+1}^{(n+1)}}\sum_{l=0}^{n}\hat{e}_l^{(n+1)}\|\tilde{u}_l\| + \frac{1}{e_{n+1}^{(n+1)}}\|f_{n+\sigma}\| \\
&= \|\frac{(1-\sigma)}{\sigma}\tilde{u}_n\| + \frac{1}{e_{n+1}^{(n+1)}}\sum_{l=0}^{n-1}-e_l^{(n+1)}\|\tilde{u}_l\| + \frac{1}{e_{n+1}^{(n+1)}}(-e_n^{(n+1)} - \frac{e_{n+1}^{(n+1)}}{\sigma}(1-\sigma))\|\tilde{u}_n\| + \frac{1}{e_{n+1}^{(n+1)}}\|f_{n+\sigma}\| \\
&= \frac{1}{e_{n+1}^{(n+1)}}\sum_{l=0}^{n}-e_l^{(n+1)}\|\tilde{u}_l\| + \frac{1}{e_{n+1}^{(n+1)}}\|f_{n+\sigma}\| \\
&\leq \frac{1}{e_{n+1}^{(n+1)}}\|f_{n+\sigma}\|\exp\left(2\tau\sum_{l=0}^{n}-e_l^{(n+1)}\right) \\
&= \frac{1}{e_{n+1}^{(n+1)}}\|f_{n+\sigma}\|\exp(2\tau e_{n+1}^{(n+1)}) \\
&\leq C_1 \max_{0\leq n\leq n_t}\|f_{n+\sigma}\|,
\end{aligned}
\tag{3.22}
$$

which confirms our assertion with $C = \max\{C_0, C_1\}$. $\qquad\square$

Theorem 3.3. *Assume that u_{n+1} and $\tilde{u}_{n+1}$ are the exact and approximate solutions of problem (1.1), respectively. Then, relation (3.6) is convergent with $O(\tau^2)$.*

Proof. Subtraction of relations (3.6) and (3.5), results in

$$
\sum_{l=0}^{n+1} e_l^{(n+1)}\left(u_l - \tilde{u}_l\right) - \Delta\left(\sigma\left(u_{n+1} - \tilde{u}_{n+1}\right) + (1-\sigma)\left(u_n - \tilde{u}_n\right)\right) + \sigma\left(u_{n+1} - \tilde{u}_{n+1}\right) + (1-\sigma)\left(u_n - \tilde{u}_n\right) = \xi_\alpha^n. \tag{3.23}
$$

By definition of $q_n = u_n - \tilde{u}_n$ and its replacement in relation (3.23), we get

$$
\sum_{l=0}^{n+1} e_l^{(n+1)} q_l - \Delta\left(\sigma q_{n+1} + (1-\sigma)q_n\right) + \sigma q_{n+1} + (1-\sigma)q_n = \xi_\alpha^n. \tag{3.24}
$$

From the inner product $\sigma q_{n+1} + (1-\sigma)q_n$ in (3.24), one obtains

$$
\begin{aligned}
\sum_{l=0}^{n+1} e_l^{(n+1)}\int_\Omega q_l(\sigma q_{n+1} + (1-\sigma)q_n)d\mathbf{x} &- \int_\Omega \Delta\left(\sigma q_{n+1} + (1-\sigma)q_n\right)(\sigma q_{n+1} + (1-\sigma)q_n)d\mathbf{x} \\
&+ \|\sigma q_{n+1} + (1-\sigma)q_n\|^2 = \int_\Omega \xi_\alpha^n(\sigma q_{n+1} + (1-\sigma)q_n)d\mathbf{x}.
\end{aligned}
\tag{3.25}
$$

Employing divergence theorem and using $\|\sigma q_{n+1} + (1-\sigma)q_n\|^2, \|\nabla\left(\sigma q_{n+1} + (1-\sigma)q_n\right)\|^2 \geq 0$, we get

$$
\sum_{l=0}^{n+1} e_l^{(n+1)}\int_\Omega q_l(\sigma q_{n+1} + (1-\sigma)q_n)d\mathbf{x} \leq \int_\Omega \xi_\alpha^n(\sigma q_{n+1} + (1-\sigma)q_n)d\mathbf{x}. \tag{3.26}
$$

8

Also, we have

$$e_{n+1}^{(n+1)}\left\langle q_{n+1}, \sigma q_{n+1}+(1-\sigma)q_n \right\rangle \leq -\sum_{l=0}^{n} e_l^{(n+1)} \int_{\Omega} q_l(\sigma q_{n+1}+(1-\sigma)q_n)d\mathbf{x}+\int_{\Omega} \xi_\alpha^n(\sigma q_{n+1}+(1-\sigma)q_n)d\mathbf{x}. \quad (3.27)$$

Using the Cauchy-Schwarz inequality and relation (3.16), results in

$$\frac{e_{n+1}^{(n+1)}}{\sigma}\|\sigma q_{n+1}\|^2 - \frac{e_{n+1}^{(n+1)}}{\sigma}\|(1-\sigma)q_n\|^2 \leq \left(\sum_{l=0}^{n} \hat{e}_l^{(n+1)}\|q_l\| + \|\xi_\alpha^n\|\right)\left(\|\sigma q_{n+1}+(1-\sigma)q_n\|\right), \quad (3.28)$$

or equivalently,

$$\begin{aligned}
\|q_{n+1}\| &\leq \|\frac{(1-\sigma)}{\sigma}q_n\| + \frac{1}{e_{n+1}^{(n+1)}}\sum_{l=0}^{n}\hat{e}_l^{(n+1)}\|q_l\| + \frac{1}{e_{n+1}^{(n+1)}}\|\xi_\alpha^n\| \\
&\leq \|\frac{(1-\sigma)}{\sigma}q_n\| + \frac{1}{e_{n+1}^{(n+1)}}\sum_{l=0}^{n}\hat{e}_l^{(n+1)}\|q_l\| + \frac{1}{e_{n+1}^{(n+1)}}C\tau^{3-\alpha_{\max}}.
\end{aligned} \quad (3.29)$$

In the case of $n=0$, we have

$$\|q_1\| \leq \|q_0\| + \frac{1}{e_{n+1}^{(n+1)}}C\tau^{3-\alpha_{\max}} = \frac{1}{e_{n+1}^{(n+1)}}C\tau^{3-\alpha_{\max}} \leq \mathfrak{C}_0\tau^{3-\alpha_{\max}}, \quad (3.30)$$

and for $n=1,\cdots,n_t$, it yields

$$\begin{aligned}
\|q_{n+1}\| &\leq \|\frac{(1-\sigma)}{\sigma}q_n\| + \frac{1}{e_{n+1}^{(n+1)}}\sum_{l=0}^{n}\hat{e}_l^{(n+1)}\|q_l\| + \frac{1}{e_{n+1}^{(n+1)}}C\tau^{3-\alpha_{\max}} \\
&\leq \frac{1}{e_{n+1}^{(n+1)}}C\tau^{3-\alpha_{\max}}\exp\left(2\tau\sum_{l=0}^{n}-e_l^{(n+1)}\right) \\
&= \frac{1}{e_{n+1}^{(n+1)}}C\tau^{3-\alpha_{\max}}\exp(2\tau e_{n+1}^{(n+1)}) \\
&\leq \mathfrak{C}_1\tau^{3-\alpha_{\max}}.
\end{aligned} \quad (3.31)$$

Since the $0 < \alpha \leq 1$, this completes the proof. □

4. The MK interpolation

The MK interpolation method is used in order to construct shape function and its derivatives while satisfies the Kronecker delta condition. For this purpose, the domain Ω of problem (1.1) is discretized with n' scattered points. Assuming that $\Omega_{\mathbf{x}}$ is a sub-domain of Ω in the neighborhood of point $\mathbf{x}$ and contains $N(\leq n')$ points. So, the MK interpolation $u^h(\mathbf{x})$ is defined as follows

$$u^h(\mathbf{x}) = \sum_{i=1}^{N}\phi_i(\mathbf{x})u_i = \Phi(\mathbf{x})\mathbf{u} = \left(p^T(\mathbf{x})\mathcal{A} + r^T(\mathbf{x})\mathcal{B}\right)\mathbf{u}, \qquad \mathbf{x}\in\Omega_{\mathbf{x}}, \quad (4.1)$$

9

where $\Phi(\mathbf{x})$ are the shape functions and matrices $\mathcal{A}$ and $\mathcal{B}$ are obtained as

$$\begin{cases} \mathcal{A} = (P^T R^{-1} P)^{-1} P^T R^{-1}, \\ \mathcal{B} = R^{-1}(I - P\mathcal{A}), \end{cases} \tag{4.2}$$

in which, I is an unit matrix and the entries of $(N \times m)$-matrix P are computed as

$$P = \begin{bmatrix} p_1(\mathbf{x}_1) & \cdots & p_m(\mathbf{x}_1) \\ \cdots & \cdots & \cdots \\ p_1(\mathbf{x}_N) & \cdots & p_m(\mathbf{x}_N) \end{bmatrix}, \tag{4.3}$$

where $p(\mathbf{x})$ is a vector of complete monomial basis of order m as

$$p^T(\mathbf{x}) = [p_1(\mathbf{x}), p_2(\mathbf{x}), \dots, p_m(\mathbf{x})], \tag{4.4}$$

and according to the dimension of the problem is as follows

$$p^T(\mathbf{x}) = \left[1, x, x^2, x^3, x^4\right], \qquad m = 5,$$

or

$$p^T(\mathbf{x}) = \left[1, x, y, x^2, xy, y^2, x^3, x^2 y, xy^2, y^3, x^4, x^3 y, x^2 y^2, xy^3, y^4\right], \qquad m = 15.$$

Moreover, R and $r(\mathbf{x})$ in relations (4.1) and (4.2) are given by

$$R = \begin{bmatrix} r(\mathbf{x}_1, \mathbf{x}_1) & \cdots & r(\mathbf{x}_1, \mathbf{x}_N) \\ \cdots & \cdots & \cdots \\ r(\mathbf{x}_N, \mathbf{x}_1) & \cdots & r(\mathbf{x}_N, \mathbf{x}_N) \end{bmatrix}, \tag{4.5}$$

and

$$\mathbf{r}^T(\mathbf{x}) = [\lambda(\mathbf{x}, \mathbf{x}_1) \dots \lambda(\mathbf{x}, \mathbf{x}_N)], \tag{4.6}$$

where $\lambda(\mathbf{x}, \mathbf{x}_j)$ is called the correlation function and is adopted as

$$\lambda(\mathbf{x}, \mathbf{x}_i) = \begin{cases} 1 - 6s_i^2 + 8s_i^3 - 3s_i^4, & s_i \leq 1, \\ 0, & s_i > 1, \end{cases} \tag{4.7}$$

in which $s_i = \frac{\|\mathbf{x} - \mathbf{x}_i\|}{r_i}$ and r_i is the size of support in the weight function.

5. Construction of the method

In this part, we establish a hybrid local collocation method based on the MK interpolation and finite difference method to solve the problem (1.1). To do this, we review the relation (3.5) as

$$\sum_{l=0}^{n} d_l^{(n+1)} \left(\tilde{u}_{n-l+1} - \tilde{u}_{n-l}\right) - \Delta\left(\sigma \tilde{u}_{n+1} + (1-\sigma)\tilde{u}_n\right) + \sigma \tilde{u}_{n+1} + (1-\sigma)\tilde{u}_n = f_{n+\sigma}, \tag{5.1}$$

10

or equivalently,

$$d_0^{(n+1)}\tilde{u}_{n+1} - \sigma\left(\Delta\tilde{u}_{n+1} - \tilde{u}_{n+1}\right) = d_0^{(n+1)}\tilde{u}_n + (1-\sigma)\left(\Delta\tilde{u}_n - \tilde{u}_n\right) - \sum_{l=1}^{n} d_l^{(n+1)}\left(\tilde{u}_{n-l+1} - \tilde{u}_{n-l}\right) + f_{n+\sigma}. \quad (5.2)$$

So, the discretization in time variable is finished. To discretizate Eq (5.2) in space variables, we choose several random distribution points such as $\{\mathbf{x}_1, \mathbf{x}_2, \ldots, \mathbf{x}_{n'}\}$ in the problem domain Ω. Note that these nodes must suitably spread in the domain. Now, regarding a subdomain around each node, these subdomains can be of any preferred geometric shapes [36]. In addition, these subdomains overlap each other and cover the whole problem domain. For every arbitrary point $\mathbf{x}_s$, we present the local weak form of (5.2) related to subdomain $\Omega_{\mathbf{x}_s}$ of $\mathbf{x}_s$ as

$$d_0^{(n+1)}\tilde{u}_{n+1}(\mathbf{x}_s) - \sigma\left(\Delta\tilde{u}_{n+1}(\mathbf{x}_s) - \tilde{u}_{n+1}(\mathbf{x}_s)\right) = d_0^{(n+1)}\tilde{u}_n(\mathbf{x}_s) + (1-\sigma)\left(\Delta\tilde{u}_n(\mathbf{x}_s) - \tilde{u}_n(\mathbf{x}_s)\right)$$
$$- \sum_{l=1}^{n} d_l^{(n+1)}\left(\tilde{u}_{n-l+1}(\mathbf{x}_s) - \tilde{u}_{n-l}(\mathbf{x}_s)\right) + f_{n+\sigma}(\mathbf{x}_s), \quad (5.3)$$

in which $\tilde{u}_n(\mathbf{x}_s) = \tilde{u}(\mathbf{x}_s, n\tau)$. Now, suppose that there are only N points around $\mathbf{x}_s$. So, using (4.1), the following MK interpolation for $\tilde{u}$ in Ω_s is resulted

$$\tilde{u}^h(\mathbf{x}, t) = \sum_{j=1}^{N} \phi_j(\mathbf{x})\hat{\tilde{u}}_j = \Phi(\mathbf{x})\tilde{\mathbf{u}}(t), \quad \mathbf{x} \in \Omega_{\mathbf{x}_s}. \quad (5.4)$$

By duplicating this strategy for all points, the following matrix procedure will be obtained

$$\mathbf{K}\tilde{\mathbf{U}}_{n+1} = \tilde{\mathbf{K}}\tilde{\mathbf{U}}_n - \sum_{l=1}^{n} d_l^{(n+1)}\mathbf{C}\left(\tilde{\mathbf{U}}_{n-l+1} - \tilde{\mathbf{U}}_{n-l}\right) + \tilde{\mathbf{F}}_{n+\sigma}, \quad (5.5)$$

in which $\tilde{\mathbf{F}}_{n+\sigma} = [f(\mathbf{x}_1, (n+\sigma)\tau), \ldots, f(\mathbf{x}_{n'}, (n+\sigma)\tau)]^T$ and $\tilde{\mathbf{U}}_{n+1} = [\tilde{u}(\mathbf{x}_1, (n+1)\tau), \ldots, \tilde{u}(\mathbf{x}_{n'}, (n+1)\tau)]^T$.

Also, the elements of these matrices are calculated as follows

$$\mathbf{C}_{ij} = \psi_i(\mathbf{x}_j), \quad \mathbf{K}_{ij} = d_0^{(n+1)}\psi_i(\mathbf{x}_j) - \sigma(\Delta\psi_i(\mathbf{x}_j) - \psi_i(\mathbf{x}_j)), \quad \mathbf{F}_i = f(\mathbf{x}_i, (n+\sigma)\tau),$$
$$\tilde{\mathbf{K}}_{ij} = d_0^{(n+1)}\psi_i(\mathbf{x}_j) + (1-\sigma)(\Delta\psi_i(\mathbf{x}_j) - \psi_i(\mathbf{x}_j)).$$

Therefore, the full discretization of the problem is constructed. To explain the capability of the presented method, some examples are considered in the next section.

6. Numerical results

In this section, some numerical examples are studied to examine the efficiency of the presented method. To investigate the capability of the established method, the problem errors are computed as follows

$$L_\infty = \|u(\mathbf{x}, T) - \tilde{u}_{n_t}(\mathbf{x}, T)\|_\infty = \max_{\mathbf{x} \in \Omega} |u(\mathbf{x}, T) - \tilde{u}_{n_t}(\mathbf{x}, T)|,$$

$$L_2 = \|u(\mathbf{x}, T) - \tilde{u}_{n_t}(\mathbf{x}, T)\|_2 = \left(\int_\Omega (u(\mathbf{x}, T) - \tilde{u}_{n_t}(\mathbf{x}, T))^2 d\mathbf{x} \right)^{\frac{1}{2}},$$

and

$$\|u(\mathbf{x}, T) - \tilde{u}_{n_t}(\mathbf{x}, T)\|_{RMS} = \sqrt{\frac{\sum_{i=1}^{M} \left(u(\mathbf{x}, T) - \tilde{u}_{n_t}(\mathbf{x}, T) \right)^2}{M}}.$$

Moreover, to show validity of the method, the time variable order is calculated as

$$Co = \frac{\log\left(\frac{E_1}{E_2}\right)}{\log\left(\frac{\tau_1}{\tau_2}\right)}, \tag{6.1}$$

where E_1 and E_2 are errors related to τ_1 and τ_2, respectively.

EXAMPLE 1. For the first example, we study the following model in one dimensional case

$$\int_0^1 \varpi(\alpha) \, {}_0^c D_t^\alpha u(x, t) d\alpha - \frac{\partial^2 u(x, t)}{\partial x^2} + u(x, t) = f(x, t), \qquad x \in [0, 1], \tag{6.2}$$

in which $\varpi(\alpha) = \Gamma(5 - \alpha)$. The exact solution is $u(x, t) = t^4 \sin(x)$ and the initial and Dirichlet boundary conditions are as follows

$$\begin{cases} u(x, 0) = 0, & \text{initial condition}, \\ u(0, t) = 0, \quad u(1, t) = t^4 \sin(1), & \text{boundary condition}. \end{cases}$$

We obtain the source term f from the exact solution. Table 1 reports the calculation at $T = 1$ with employing 21 uniform nodes in $[0, 1]$. Based on the calculation connected to the rates of convergence, we conclude that the order is almost $O(\tau^2)$. Ona can see that the computational results are agreement with the theoretical results of Theorem 3.3. The outcomes of this table illustrate that the presented numerical procedure is feasible and effective in one dimension case.

Figure 2 (left) depicts the absolute error for this example at various final times. Furthermore, the exact and numerical solutions are depicted in Figure 2 (Right). Figure 2 and Table 1 reveal that the presented method has good accuracy to obtain the numerical solution of this problem in one dimension case.
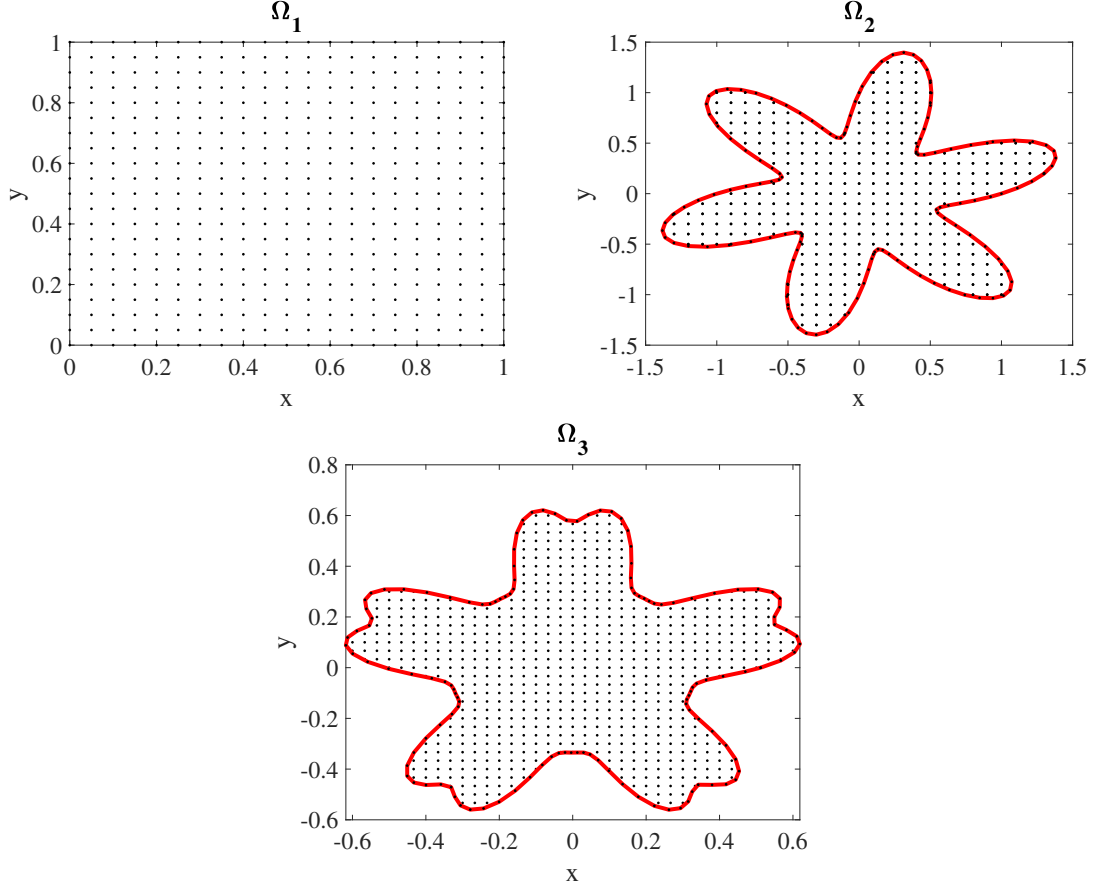
12

Fig. 1: The regular and irregular problem domains.

Table 1: The L_2, L_∞ and RMS errors and related convergence orders for Example 1 over Ω_1 with $T = 1$.

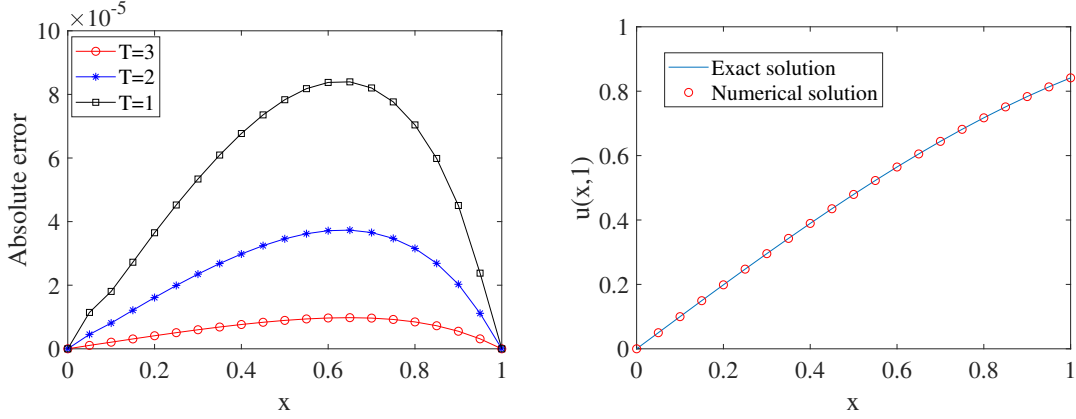| τ	L_2	Co	L_∞	Co	RMS	Co
0.0400	$5.5332E-04$	–	$1.7400E-04$	–	$1.2074E-04$	–
0.0200	$1.3105E-04$	2.0780	$4.1215E-05$	2.0778	$2.8598E-05$	2.0779
0.0100	$3.1130E-05$	2.0737	$9.7918E-06$	2.0735	$6.7931E-06$	2.0738
0.0050	$7.4414E-06$	2.0647	$2.3419E-06$	2.0639	$1.6238E-06$	2.0647
0.0025	$1.7982E-06$	2.0490	$5.6693E-07$	2.0464	$3.9241E-07$	2.0489

13

Fig. 2: The graph of absolute error (left) for $T = 1, 2, 3$, and graph of the exact and approximate solutions (right) for Example 1 at $T = 1$ with $\tau = 0.0200$.

EXAMPLE 2. Consider the following equation

$$\int_0^1 \Gamma(3-\alpha)\, {}_0^c D_t^\alpha u(\mathbf{x}, t) d\alpha - \Delta u(\mathbf{x}, t) + u(\mathbf{x}, t) = t^2 \sin(x) \sin(y) \left(\frac{2}{\ln t}(1 - \frac{1}{t}) + 3 \right), \qquad (6.3)$$

subject to the homogeneous initial and boundary conditions as

$$\begin{cases} u(0, y, t) = 0, & u(1, y, t) = t^2 \sin(1) \sin(y), \\ u(x, 0, t) = 0, & u(x, 1, t) = t^2 \sin(x) \sin(1). \end{cases}$$

The global domain is a square $\Omega_1 = [0, 1] \times [0, 1]$ in Figure 1. We use 361 uniform nodes in the interior of Ω_1 and 80 nodes in the boundary $\partial\Omega_1$. Also, the final time is $T = 1$ and the analytical solution is as follows

$$u(x, y, t) = t^2 \sin(x) \sin(y). \qquad (6.4)$$

We compute the L_2, L_∞ and RMS errors between the exact and numerical solutions and list the results in Table 2. Using the results of this table, the convergence order is almost $O(\tau^2)$. This fact confirms that the computational results support the theoretical results of Theorem 3.3.

Figure 3 shows the absolute error and approximate solution of Example 2. The step time and final time are $\tau = 0.005$ and $T = 1$, respectively. According to Figure 3 and Table 2, the presented method has good accuracy to obtain the numerical approximation of this example.

EXAMPLE 3. We consider the following model

$$\int_0^1 \varpi(\alpha)\, {}_0^c D_t^\alpha u(\mathbf{x}, t) d\alpha - \Delta u(\mathbf{x}, t) + u(\mathbf{x}, t) = f(\mathbf{x}, t), \qquad \mathbf{x} = (x, y) \in \Omega_2, \qquad (6.5)$$

14

Table 2: The L_2, L_∞ and RMS errors and related convergence orders for Example 2 over Ω_1 with $T = 1$.

τ	L_2	Co	L_∞	Co	RMS	Co
0.0400	$1.9453E - 04$	$-$	$1.9021E - 05$	$-$	$9.2635E - 06$	$-$
0.0200	$4.9613E - 05$	1.9712	$4.8655E - 06$	1.9669	$2.3625E - 06$	1.9712
0.0100	$1.2849E - 05$	1.9491	$1.2705E - 06$	1.9372	$6.1185E - 07$	1.9491
0.0050	$3.6965E - 06$	1.7974	$3.6158E - 07$	1.8130	$1.7602E - 07$	1.7974
0.0025	$8.6241E - 07$	2.0997	$9.0215E - 08$	2.0029	$4.1067E - 08$	2.0997

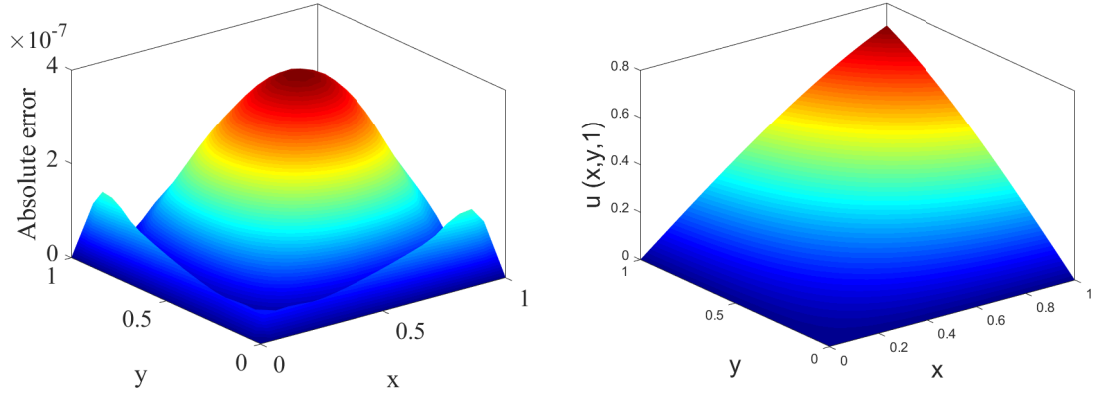
Fig. 3: The graph of absolute error (left) and approximate solution (right) for Example 2 at $T = 1$ with $\tau = 0.005$.

Table 3: The L_2, L_∞ and RMS errors and related convergence orders for Example 3 over Ω_2 with $T = 1$.

τ	L_2	Co	L_∞	Co	RMS	Co
$1/200$	$8.8730E-06$	$-$	$1.0072E-06$	$-$	$4.1015E-07$	$-$
$1/300$	$3.9574E-06$	1.9914	$4.4920E-07$	1.9914	$1.8243E-07$	1.9981
$1/400$	$2.2308E-06$	1.9926	$2.5322E-07$	1.9925	$1.0312E-07$	1.9830
$1/500$	$1.4299E-06$	1.9931	$1.6201E-07$	2.0014	$6.6097E-08$	1.9932
$1/600$	$9.9010E-07$	2.0160	$1.1204E-07$	2.0228	$4.5901E-08$	2.0000

with the analytical solution $u(x, y, t) = t^2(x^3 + y^3)$ and $\varpi(\alpha) = \Gamma(3 - \alpha)$. Also, the initial condition, Dieichlet boundary conditions and the function f can be extracted from the exact solution. The global domain is irregular shape Ω_2 in Figure 1. Moreover, the boundary of global domain has the following parametric formula

$$\left\{ (x, y) \in \mathbb{R}^2 : x = r\cos(\theta), y = r\sin(\theta), \quad \theta \in [0, 2\pi], \qquad r = 1 + \tanh(\cos(n_1\theta))\sin(n_2\theta) \right\}, \qquad (6.6)$$

in which $n_1 = n_2 = 3$. The number of interior and boundary points are 342 and 126, respectively. Table 3 demonstrates the numerical results for Example 3. These results confirm that the convergence order is almost $O(\tau^2)$. This issue proves that the computational outcomes keep the theoretical results of Theorem 3.3. Figure 4 displays the absolute errors and numerical solutions on irregular domains. The results of Table 3 and Figure 4 indicate that the presented method has good convergence order and are agreement with the exact solution.

EXAMPLE 4. In this example, we assume the following model

$$\int_0^1 \varpi(\alpha) \, {}^c_0 D_t^\alpha u(\mathbf{x}, t) d\alpha - \Delta u(\mathbf{x}, t) + u(\mathbf{x}, t) = t^3 e^{x+y} \left(\frac{6}{\ln t}(1 - \frac{1}{t}) - 1 \right), \qquad (6.7)$$

in which $\varpi(\alpha) = \Gamma(4 - \alpha)$ and the global domain is Ω_3 (see Figure 1). The boundary of this domain has the following parametric formula

$$\left\{ (x, y) \in \mathbb{R}^2 : x = r\cos(\theta), y = r\sin(\theta), \quad \theta \in [0, 2\pi], \qquad r = 0.5\sqrt{\sin(5\theta) + (1.1 - \sin(5\theta)^{3/2})} \right\}. \quad (6.8)$$

We apply 126 points in boundary and 704 nodes in the global domain Ω_3. The analytical solution is $u(x, y, t) = t^3 e^{x+y}$. Also, the initial and boundary conditions are obtained by these information's.

The first column of Table 4 is step time which decreases at each stage. In columns 2 , 4 and 6, we have L_2, L_∞ and RMS errors and related convergence orders at $T = 1$. This table illustrates that the presented numerical scheme has almost $O(\tau^2)$ convergence order and shows that the computational results are confirmed to the theoretical results of Theorem 3.3.
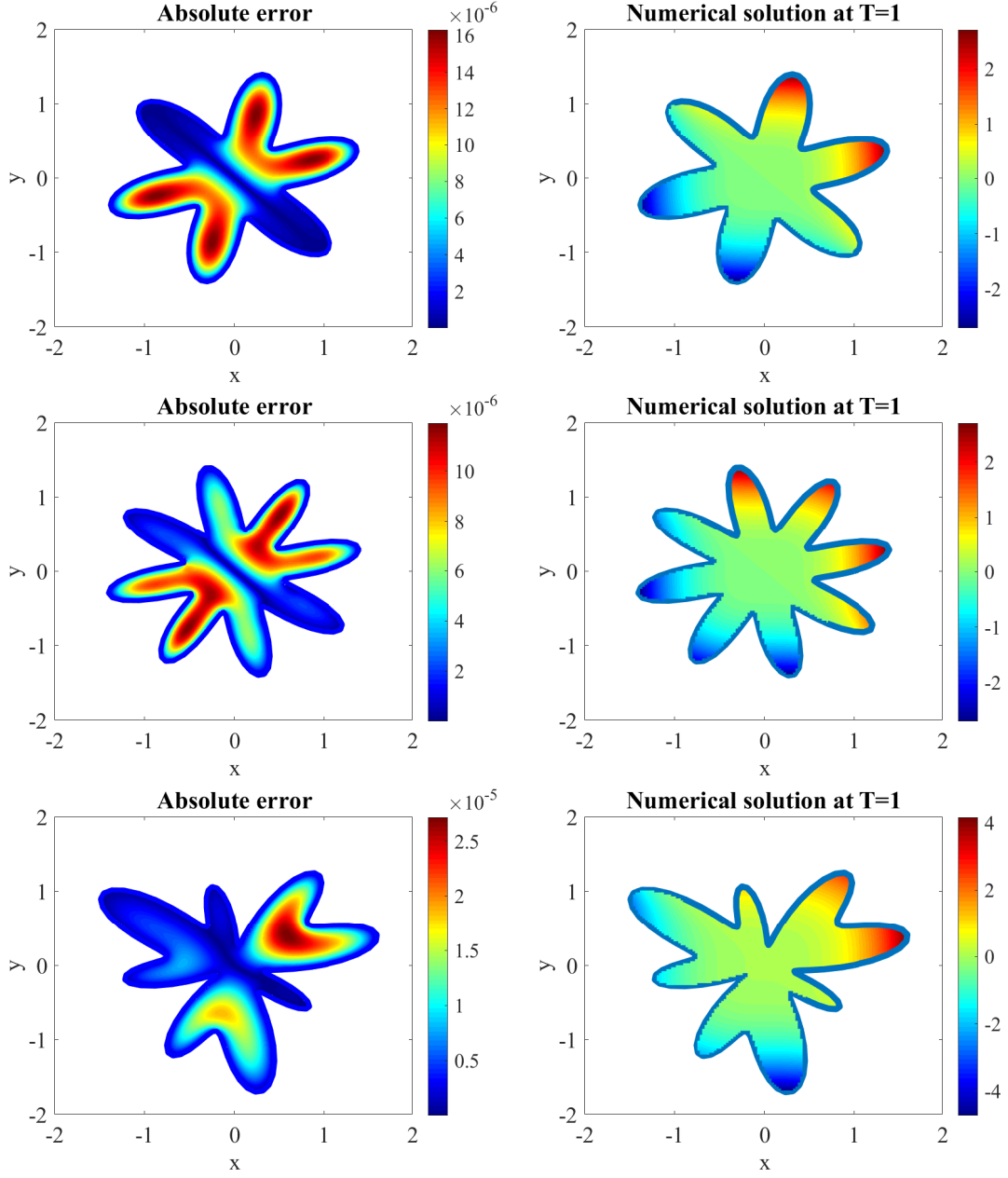
Fig. 4: The absolute error (left) and approximate solution (right) on irregular domains for Example 3 at $T = 1$ with $\tau = 0.005$.
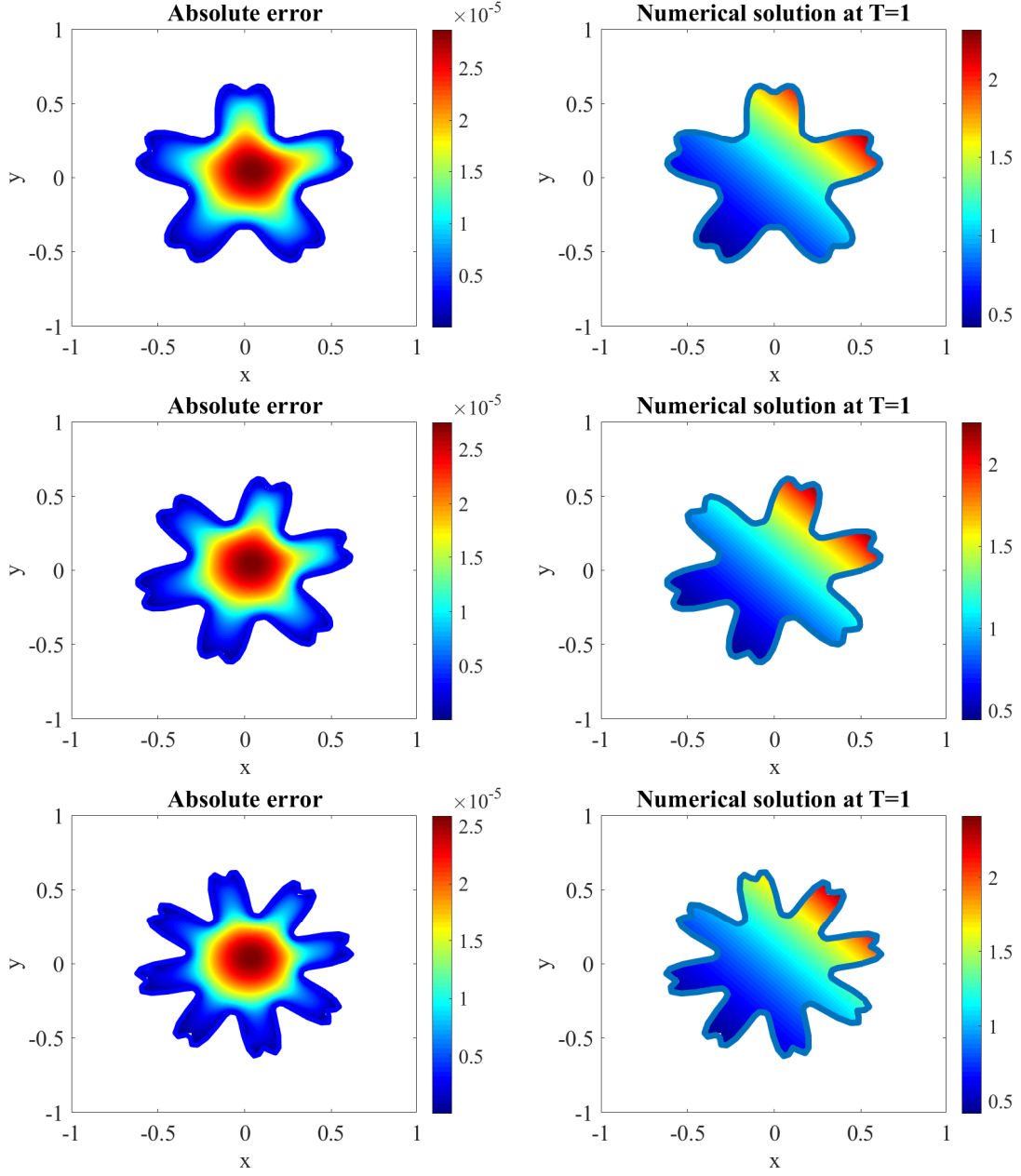
Fig. 5: The absolute error (left) and approximate solution (right) on irregular domains for Example 4 at $T = 1$ with $\tau = 0.005$.

Table 4: The L_2, L_∞ and RMS errors and related convergence orders for Example 4 over Ω_3 with $T = 1$.

τ	L_2	Co	L_∞	Co	RMS	Co
0.0400	$5.2831E - 04$	–	$2.8456E - 05$	–	$1.6264E - 05$	–
0.0200	$1.2902E - 04$	2.0338	$7.7328E - 06$	1.8797	$3.9719E - 06$	2.0338
0.0100	$3.1617E - 05$	2.0288	$2.0600E - 06$	1.9083	$9.7335E - 07$	2.0288
0.0050	$7.9591E - 06$	1.9900	$5.1789E - 07$	1.9919	$2.4503E - 07$	1.9900
0.0025	$1.9478E - 06$	2.0308	$1.2185E - 07$	2.0875	$5.9965E - 08$	2.0308

Figure 5 represents the approximate solution and related absolute error on different irregular domains at $T = 1$ with time step $\tau = 0.0400$. From the outcomes of Table 4 and Figure 5, one observes that the current numerical procedure has good accuracy and is efficient in the irregular domain for solving this example.

7. Conclusion

In this work, a flexible local collocation meshless method was used for the numerical solution of distributed order time-fractional reaction-diffusion equation. The Moving Kriging interpolation and $L2 - 1_\sigma$ method with the Gauss-Legendre numerical integration were employed to deal with this problem. Also, the unconditionally stability and convergence of the proposed technique were investigated. Numerical results illustrated that the order of convergence of this scheme confirmed the theoretical results. Some examples were studied and they showed the accuracy and capability of the presented algorithm for solving such problems.

References

References

[1] S. Guo, L. Mei, Y. Li, and Y. Sun. The improved fractional sub-equation method and its applications to the space–time fractional differential equations in fluid mechanics. *Physics Letters A*, 376(4):407–411, 2012.

[2] B. Lohana, K. A. Abro, and A. W. Shaikh. Thermodynamical analysis of heat transfer of gravity-driven fluid flow via fractional treatment: an analytical study. *Journal of Thermal Analysis and Calorimetry*, 144(1):155–165, 2021.

[3] J. F. Gómez-Aguilar, M. G. López-López, V. M. Alvarado-Martínez, J. Reyes-Reyes, and M. Adam-Medina. Modeling diffusive transport with a fractional derivative without singular kernel. *Physica A: Statistical Mechanics and its Applications*, 447:467–481, 2016.

[4] M. S. Sarafraz and M. S. Tavazoei. Realizability of fractional-order impedances by passive electrical networks composed of a fractional capacitor and rlc components. *IEEE Transactions on Circuits and Systems I: Regular Papers*, 62(12):2829–2835, 2015.

[5] R. Kopka and W. Tarczyński. A fractional model of supercapacitors for use in energy storage systems of next-generation shipboard electrical networks. *Journal of Marine Engineering & Technology*, 16(4):200–208, 2017.

[6] J. Gulgowski and T. P. Stefański. On applications of fractional derivatives in electromagnetic theory. In *2020 23rd International Microwave and Radar Conference (MIKON)*, pages 13–17. IEEE, 2020.

[7] D. H. Werner and R. Mittra. Fractional paradigm in electromagnetic theory. 2000.

[8] E. A. Abdel-Rehim. The approximate and analytic solutions of the time-fractional intermediate diffusion wave equation associated with the fokker–planck operator and applications. *Axioms*, 10(3):230, 2021.

[9] M. Mohammad, A. Trounev, and M. Alshbool. A novel numerical method for solving fractional diffusion-wave and nonlinear fredholm and volterra integral equations with zero absolute error. *Axioms*, 10(3):165, 2021.

[10] N. Ahmed, J. E. Macías-Díaz, A. Raza, D. Baleanu, M. Rafiq, Z. Iqbal, and M. O. Ahmad. Design, analysis and comparison of a nonstandard computational method for the solution of a general stochastic fractional epidemic model. *Axioms*, 11(1):10, 2022.

[11] G. Dong and M. Deng. Gpu based modelling and analysis for parallel fractional order derivative model of the spiral-plate heat exchanger. *Axioms*, 10(4):344, 2021.

[12] S. Asawasamrit, Y. Thadang, S. K. Ntouyas, and J. Tariboon. Non-instantaneous impulsive boundary value problems containing caputo fractional derivative of a function with respect to another function and riemann–stieltjes fractional integral boundary conditions. *Axioms*, 10(3):130, 2021.

[13] C. Kiataramkul, W. Yukunthorn, S. K. Ntouyas, and J. Tariboon. Sequential riemann–liouville and hadamard–caputo fractional differential systems with nonlocal coupled fractional integral boundary conditions. *Axioms*, 10(3):174, 2021.

[14] W. Bu, Y. Tang, Y. Wu, and J. Yang. Finite difference/finite element method for two-dimensional space and time fractional bloch–torrey equations. *Journal of Computational Physics*, 293:264–279, 2015.

[15] M. H. Heydari, M. R. Hooshmandasl, and F. M. M. Ghaini. An efficient computational method for solving fractional biharmonic equation. *Computers & Mathematics with Applications*, 68(3):269–287, 2014.

[16] M. H. Heydari, M. R. Hooshmandasl, F. M. M. Ghaini, and C. Cattani. Wavelets method for solving fractional optimal control problems. *Applied Mathematics and Computation*, 286:139–154, 2016.

[17] M. H. Heydari, M. R. Hooshmandasl, F. Mohammadi, and C. Cattani. Wavelets method for solving systems of nonlinear singular fractional volterra integro-differential equations. *Communications in Nonlinear Science and Numerical Simulation*, 19(1):37–48, 2014.

[18] Y. Li, H. Sheng, and Y. Q. Chen. On distributed order integrator/differentiator. *Signal Processing*, 91(5):1079–1084, 2011.

[19] M. A. Zaky and J. A. T. Machado. On the formulation and numerical simulation of distributed-order fractional optimal control problems. *Communications in Nonlinear Science and Numerical Simulation*, 52:177–189, 2017.

[20] M. Caputo. Mean fractional-order-derivatives differential equations and filters. *Annali dell'Universita di Ferrara*, 41(1):73–84, 1995.

[21] R. L. Bagley and P. J. Torvik. On the existence of the order domain and the solution of distributed order equations-part i. *International Journal of Applied Mathematics*, 2(7):865–882, 2000.

[22] R. L. Bagley and P. J. Torvik. On the existence of the order domain and the solution of distributed order equations-part ii. *International Journal of Applied Mathematics*, 2(8):965–988, 2000.

[23] Y. A. Rossikhin and M. V. Shitikova. Applications of fractional calculus to dynamic problems of linear and nonlinear hereditary mechanics of solids. 1997.

[24] Z. Jiao, Y. Chen, and I. Podlubny. Distributed order dynamic systems, modeling, analysis and simulation, 2012.

[25] J. Li, F. Liu, L. Feng, and I. Turner. A novel finite volume method for the riesz space distributed-order diffusion equation. *Computers & Mathematics with Applications*, 74(4):772–783, 2017.

[26] K. Diethelm and N. J. Ford. Numerical analysis for distributed-order differential equations. *Journal of Computational and Applied Mathematics*, 225(1):96–104, 2009.

[27] J. Ren and H. Chen. A numerical method for distributed order time fractional diffusion equation with weakly singular solutions. *Applied Mathematics Letters*, 96:159–165, 2019.

[28] S. Guo, Y. Chen, L. Mei, and Y. Song. Finite difference/generalized hermite spectral method for the distributed-order time-fractional reaction-diffusion equation on multi-dimensional unbounded domains. *Computers & Mathematics with Applications*, 93:1–19, 2021.

[29] M. Abbaszadeh and M. Dehghan. Meshless upwind local radial basis function-finite difference technique to simulate the time-fractional distributed-order advection–diffusion equation. *Engineering with computers*, 37(2):873–889, 2021.

[30] K. Maleknejad, J. Rashidinia, and T. Eftekhari. Numerical solutions of distributed order fractional differential equations in the time domain using the müntz–legendre wavelets approach. *Numerical Methods for Partial Differential Equations*, 37(1):707–731, 2021.

[31] B. Yuttanan and M. Razzaghi. Legendre wavelets approach for numerical solutions of distributed order fractional differential equations. *Applied Mathematical Modelling*, 70:350–364, 2019.

[32] H. Ding and C. Li. A high-order algorithm for time-caputo-tempered partial differential equation with riesz derivatives in two spatial dimensions. *Journal of Scientific Computing*, 80(1):81–109, 2019.

[33] B. P. Moghaddam, J. A. T. Machado, and M. L. Morgado. Numerical approach for a class of distributed order time fractional partial differential equations. *Applied Numerical Mathematics*, 136:152–162, 2019.

[34] A. H. Bhrawy and M. A. Zaky. Numerical simulation of multi-dimensional distributed-order generalized schrödinger equations. *Nonlinear Dynamics*, 89(2):1415–1432, 2017.

[35] S. Guo, Y. Chen, L. Mei, and Y. Song. Finite difference/generalized hermite spectral method for the distributed-order time-fractional reaction-diffusion equation on multi-dimensional unbounded domains. *Computers & Mathematics with Applications*, 93:1–19, 2021.

[36] S. N. Atluri and T. Zhu. A new meshless local petrov-galerkin (mlpg) approach in computational mechanics. *Computational mechanics*, 22(2):117–127, 1998.